Theory of a carbon-oxygen-hydrogen recombination center in n-type Si

Paulo Santos[1], José Coutinho[*,1], Sven Öberg[2], Michelle Vaqueiro-Contreras[3], Vladimir P. Markevich[3], Matthew P. Halsall[3], and Anthony R. Peaker[3]

[1] Department of Physics and I3N, University of Aveiro, Campus Santiago, 3810-193 Aveiro Portugal
[2] Department of Engineering Sciences and Mathematics, Luleå University of Technology, SE-97187 Luleå, Sweden
[3] Photon Science Institute, University of Manchester, M13 9PL, UK

[*] Corresponding author: e-mail jose.coutinho@ua.pt, Phone: +351 234 247 051, Fax: +351 234 378 197

We have recently found that in-diffusion of hydrogen into n-type Si crystals containing oxygen and carbon impurities can result in the formation of powerful recombination centers (M. Vaqueiro-Contreras et al., to appear in PSS RRL). Here, we describe a combination of first-principles calculations and electrical measurements to investigate the composition, structure, electrical activity and recombination mechanism of a carbon-oxygen-hydrogen complex (COH) in Si. We found a defect comprising a carbon-oxygen complex connected to an H atom whose location depends on the charge state of the complex, and showing a calculated acceptor level at $E_v + 0.3$ eV, a few meV away from the observations.
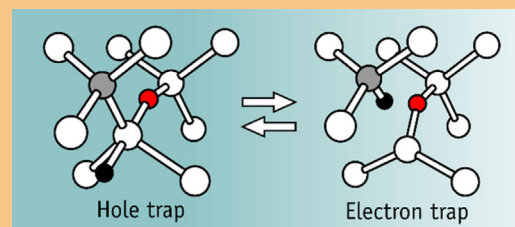
Bistable carbon–oxygen–hydrogen complex in silicon. Carbon, oxygen, hydrogen, and silicon atoms are shown in gray, red, black, and white, respectively.

1 Introduction Hydrogen, oxygen and carbon species are common contaminants in several kinds of silicon materials. Their origin is broad-based, ranging from the graphite components in the Czochralski (Cz) furnace (carbon), to the intrinsic composition of the SiO_2 crucible (oxygen), or simply, they may be unavoidable (such as hydrogen) [1–3]. Their presence is not always unintentional though. For instance, during solar cell fabrication, specific impurities are deliberately introduced, one prominent example being the deposition of a front-facing silicon nitride anti-reflection layer, which introduces large quantities of fast-diffusing atomic hydrogen into the Si [4]. This process brings important benefits, such as the reduction of surface recombination, although the underlying mechanism and possible side-effects of H injection are far from clear.

Isolated carbon and oxygen impurities in Si are electrically inert and have been subjected to extensive experimental and theoretical studies. In as-grown Cz-Si, they occur in large concentrations (usually in magnitudes of ppm atoms), normally occupying substitutional (C_s) and bond-centered interstitial (O_i) sites of the Si lattice, respectively. More than four decades ago, Newman, Willis and Bean assigned an infrared absorption band at $1104 \, \text{cm}^{-1}$ to a vibrational mode localized on a substitutional-carbon-interstitial-oxygen (CO) complex in Si [5, 6]. Combined annealing and isotope frequency shift data led the authors to the interpretation that the band resulted from the capture of a diffusing O_i impurity, which becomes mobile above $\sim 450\,°C$, by a substitutional carbon atom. These results were later supported and translated into an atomistic model by Kaneta and co-workers [7], where the O atom was not directly connected to C. Instead, C and O atoms were separated by an intermediate Si atom forming a C_s-Si-O_i unit, avoiding the formation of a C–O bond, in favor of

Phys. Status Solidi A 214, No. 7 (2017)

Original

Paper

(2 of 6) 1700309

stronger Si-O and C-Si bonds. The electronic activity of this center was not addressed at the time, but considering the coordination of the C, O, and Si-ligand atoms, the complex is expected to be electrically inactive.

Atomic hydrogen is an amphoteric impurity with negative-U ordered donor and acceptor occupancy levels at $E_c - 0.18$ eV and $\sim E_c - 0.5$ eV [8–11], respectively. It is a bistable impurity − in the positive charge state it is most stable on the site of highest electron density, that is at the bond-center site (H_{BC}^+), while in the negative charge state it avoids high electron density regions due to Coulomb repulsion, preferring to be located at the tetrahedral interstitial site (H_T^-) [3]. The neutral defect is more stable at the BC site, meaning that the donor level involves essentially a direct transition between bond-centered H_{BC}^0 and $H_{BC}^+ + e^-$ states, hereafter referred to as a $H_{BC}(0/+)$ transition, where the final state includes a free electron in the conduction band. On the other hand, the acceptor is the energy difference between H_T^- and $H_{BC}^0 + e^-$, therefore involving a considerable lattice relaxation energy. This indirect transition is referred to as $H_{T/BC}(-/0)$.

Atomic H is known to interact effectively with both carbon and oxygen impurities in Si. For the case of carbon, theory and (Laplace) deep-level transient spectroscopy (DLTS) studies agree that the most stable form of a CH complex is the one in which the H sits between the C atom and its Si first neighbor [12]. Unlike isolated bond-centered H, it was reported that the C-H-Si defect (labeled CH_{II}) shows a positive-U ordering of its donor and acceptor states at $E_v + 0.33$ eV and $E_c - 0.16$ eV, respectively [12]. An additional donor level at $E_c - 0.22$ eV (labeled CH_I) was connected to a metastable precursor of CH_{II}, and was suggested to consist on a Si-H-Si unit neighboring the C_s atom [12]. In a recent report by Stübner and co-workers [13], from the analysis of DLTS, field-induced change of emission rates, annealing and depth-profile data, it was confirmed that the $E_c - 0.16$ eV level (CH_{II} in Ref. [12], but now referred to as CH_A) is an acceptor. However, they could not find any sign of CH_I. Instead, a shallower donor transition at $E_c - 0.14$ eV (labeled CH_B) was assigned to a CH_n complex involving $n > 1$ hydrogen atoms [13].

With regards to the interaction of atomic H with O_i, we know from DLTS that the electrical levels of OH are close to those of isolated H. Accordingly, donor and acceptor occupancy transitions at $E_c - 0.17$ eV and $E_c - 0.68$ eV were assigned to OH in Si [10, 11]. Although first-principles modeling predict that hydrogen enhances oxygen diffusivity and that it does not bind directly to O [14–16], calculations of the electronic structure and electronic levels of OH in Si have not been reported so far.

We have recently reported the formation of powerful recombination centers in n-type silicon as a result of the reaction between hydrogen, carbon and oxygen species [17]. Accordingly, hole traps H_1 and H_2 at 0.38 and 0.36 eV above E_v, respectively, were detected in Cz-Si subject to wet etching, remote plasma exposure and silicon nitride deposition, and they were assigned to COH complexes. We also demonstrated that the concentration of these COH

defects is high enough to have a substantial impact on the minority carrier lifetime of Si-based solar cells.

Below we report on our latest results on the search for the atomistic and electronic details of the COH-related recombination center in Si by combining first-principles calculations with DLTS and LVM infrared absorption measurements. The next section starts with a description of the methods employed, which is followed by a summary of the key observations related to the complex. We then report on the interaction of atomic H with C and O. These results are particularly instructive. They provide us with the fundamental physical-chemical guidelines behind the model that explains the formation and properties of COH. Among the calculated observables we report binding energies, vibrational mode frequencies and electronic transitions.

2 Methods

2.1 Experimental details
For this work we selected a range of Cz and continuous Cz (CCz) n-type silicon slices with oxygen concentrations in the range $12 < [O_i] < 20$ ppma (1 ppma $= 5 \times 10^{16}$ cm^{-3}) and substitutional carbon concentration of $0.01 < [C_s] < 9$ ppma. In addition, as a control sample we included silicon grown by the float zone (FZ) method which had $[O_i]$ and $[C_s] < 0.2$ ppma. All the material was phosphorus doped with resistivities in the range 1–8 Ω-cm. The samples were hydrogenated in three different ways. Hydrogen was introduced into the samples, firstly, by wet etching with HF/HNO$_3$ solutions, secondly, by immersion in a 50 W remote H plasma for 30 min at temperatures between 25 and 250 °C, and, finally, in a way intended to simulate hydrogenation in a typical solar cell manufacturing process by in-diffusion of hydrogen from a H-rich silicon nitride film.

Schottky diodes and Ohmic contacts were fabricated on the samples prior to capacitance-voltage and DLTS measurements. Minority carrier transient spectroscopy (MCTS) [18] using a 940 nm light emitting diode for optical excitation from the back of the slice was used to determine the electronic properties of hole traps including directly measured capture cross sections used to calculate the contribution of carrier recombination at the traps to the minority carrier lifetime.

Local mode optical absorption measurements were undertaken at 30 K in the wavenumber range 500–1500 cm^{-1} in order to observe the vibrational modes of CO$_n$ complexes in the samples.

Minority carrier lifetime measurements were made using a Semilab WT-2000 PVN μ-PCD machine and iodine/ethanol surface passivation of the wafers.

2.2 Theoretical details
First-principles density functional calculations were carried out using the VASP package [19], which uses the projector-augment wave (PAW) method [20] to deal with core-electrons and planewaves with a maximum kinetic energy $E_{cut} = 370$ eV for the valence. Exchange-correlation interactions were

dealt within the generalized gradient approximation [21], and the electron density (potential) was assumed to be converged when the energy change between two consecutive self-consistent steps was less than $1\,\mu\text{eV}$.

Substitutional C, interstitial O, and interstitial H impurities were inserted into pristine 216-Si-atom supercells with cubic shape, optimized lattice constant $a = 5.4687$ Å, and respective Brillouin zones sampled over a $2 \times 2 \times 2$ grid of special $\mathbf{k}$-points. All defect structures were optimized using a quasi-Newton algorithm, until the forces acting on the atoms were converged within $0.01\,\text{eV}\,\text{Å}^{-1}$.

Electronic transitions were evaluated using the marker method [22]. Experimental levels from isolated interstitial H and from the vacancy-oxygen-hydrogen complex (VOH), were used as markers. When compared to bulk markers, these choices increase the accuracy of the calculated levels (often by about 0.1 eV) of complexes that incorporate bond-centered/tetrahedral H or a Si broken bond, respectively. The levels considered were $H_{BC}(0/+) = E_c - 0.175\,\text{eV}$, $H_{T/BC}(-/0) = E_c - 0.5\,\text{eV}$, $VOH(0/+) = E_v + 0.27\,\text{eV}$, and $VOH(-/0) = E_c - 0.32\,\text{eV}$ [8–11, 23].

LVM frequencies were obtained through diagonalization of a dynamical matrix composed of Hessian submatrices with respect to the displacement of impurity atoms plus their Si ligands. Hessian matrix elements were obtained numerically with explicit atomic displacements of 0.015 Å along all symmetry-independent directions.

3 Experimental results In MCTS and DLTS spectra of the hydrogenated oxygen and carbon rich Si samples, four electron and four hole emission peaks were detected. In the DLTS spectrum shown in Fig. 1, the peak labeled as E_4 is associated with the so-called thermal double donors originating from oxygen complexes [24], whereas the peaks E_1–E_3 are related to hydrogen complexes [25, 26].
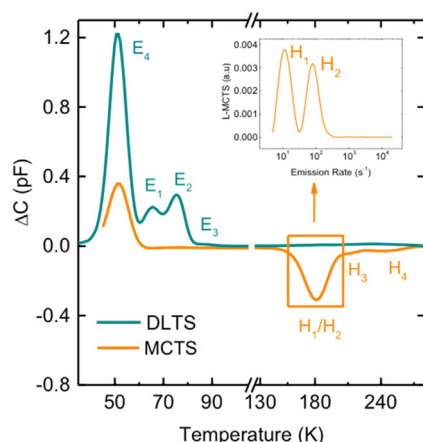

Figure 1 DLTS and MCTS spectra recorded on a sample from an n-type Cz-Si wafer, which was etched in 1HF/7HNO₃ solution for 2.5 min. We used $e_e = 50\,\text{s}^{-1}$, $U_b = -2\,\text{V}$, and $t_p = 10\,\text{ms}$ in all measurements and 940 nm LED pulses for the MCTS. The insert shows the separation of the H_1 and H_2 emission signals in the Laplace MCTS spectrum recorded at 190 K.

The E_1–E_4 traps are not significant in terms of lifetime degradation and will not be further considered in this work. The MCTS spectrum and the L-MCTS spectrum, presented as an inset in the same figure, show hole emission related signals H_1 to H_4. We have found that the dominant H_1/H_2 signals are dependent of carbon, oxygen and hydrogen content.

Firstly, we have compared the DLTS and MCTS spectra of a FZ sample with almost negligible $[O_i]$ and $[C_s]$ with the spectra for Cz and CCz samples after hydrogenation. In the FZ hydrogenated samples the H_1 and H_2 signals were not detected [27], while for the Cz and CCz samples the signals showed a proportional increase with O_i and C_s content in the crystals. Secondly, the concentration depth profiles of the H_1 and H_2 traps are found to be similar to that for the phosphorus-hydrogen complex formed in the hydrogenated samples. This provides an evidence of the involvement of a single hydrogen atom into the defects, which give rise to the H_1 and H_2 traps. Finally, a good correlation has been found between the intensity of the LVM band with its maximum at $1104\,\text{cm}^{-1}$ observed in the infrared absorption spectra of carbon and oxygen rich samples subjected to different heat-treatments in the temperature range 550–700 °C and magnitudes of the MCTS signals due to the H_1/H_2 traps in similarly heat-treated neighboring samples, which were hydrogenated and prepared for MCTS measurements [17]. The band at $1104\,\text{cm}^{-1}$ is related to an LVM of the CO complex [5, 6]. The results mentioned above give solid evidence of the carbon-oxygen-hydrogen composition of the complexes responsible for the H_1/H_2 traps.

With L-MCTS we have carried out direct measurements of electron and hole capture cross-sections and hole emission rates of the H_1 and H_2 traps. The details of the measurement technique can be found in Ref. [27]. Capture cross-section measurements of minority and majority carriers resulted respectively in values of 9.8×10^{-16} and $2.0 \times 10^{-17}\,\text{cm}^2$ for H_1, and of 7.9×10^{-16} and $1.95 \times 10^{-17}\,\text{cm}^2$ for H_2. The defect levels obtained from the Arrhenius plots of T^2-corrected hole emission rates correspond to $0.38 \pm 0.01\,\text{eV}$ and $0.36 \pm 0.01\,\text{eV}$ from the valence band for the H_1 and H_2 centers, respectively. These characteristics indicate that the defects have an acceptor-like behavior and likely to be powerful recombination centers in n-type material. Furthermore, it has been found that the H_1/H_2 traps anneal out in the temperature range from 150 to 200 °C and their elimination resulted in significant improvement of lifetime in silicon wafers (see Refs. [17] and [27]).

4 Theoretical results
4.1 Carbon–hydrogen interactions Figure 2(a) shows a substitutional carbon atom in Si with several Si ligands. It also shows some sites (black dots) among many at which we placed a hydrogen atom to investigate the relative stability of CH complexes. In agreement with Andersen et al. [12], we found that for all charge states investigated (−, 0, and +), H prefers to connect directly to the carbon atom, close to site BC1. Other low-energy structures are

Phys. Status Solidi A 214, No. 7 (2017)

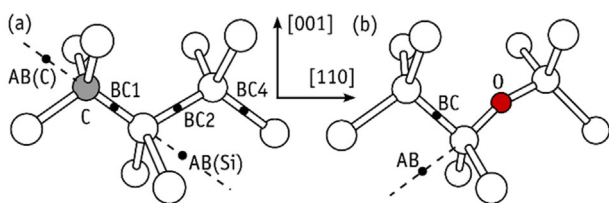Original

Paper

(4 of 6) 1700309

Figure 2 Low-energy sites (black dots), for hydrogen next to (a) substitutional carbon and (b) interstitial oxygen impurities. These diagrams are only schematic, representing approximate structures of defects obtained after atomic relaxation. C, O, and Si are represented in gray, red, and white, respectively.

BC2 and AB(C). In the neutral charge state, their energies are 0.51 and 0.64 eV above the BC1 ground state.

The formation of a short C–H bond is an important stabilization factor for CH_{BC1}, in spite of the fact that it also leaves an unsaturated radical on the nearest Si atom. This dangling bond creates a semi-occupied one-electron state deep in the gap, making VOH an excellent marker to calculate its electronic levels. Comparing ionization energies and electron affinities of CH_{BC1} with the same quantities from VOH we obtain donor and acceptor levels for CH_{BC1} at $E_v + 0.28$ eV and $E_c - 0.17$ eV, respectively, at most ~ 0.05 eV away from the transitions observed at $E_v + 0.33$ eV and $E_c - 0.16$ eV (labeled CH_{II}) [12, 13].

Also in line with Ref. [12], we found that in the positive and negative charge states the BC2 and AB(C) structures are metastable by only 0.30 and 0.23 eV, respectively. The former configuration comprises a Si-H_{BC}^+-Si unit next to C_s, and therefore it is expected to show donor activity in close resemblance to that of isolated H in Si. Here, isolated H_{BC} should be a good marker. Accordingly, we obtain a $CH_{BC2}(0/+)$ transition at $E_c - 0.24$ eV, about 0.02 eV deeper than the measured additional CH-related donor reported in Ref. [12] and labeled CH_I. It is relevant to note that the calculated $H_{BC2}(0/+)$ location is deeper than $CH_{BC1}(-/0)$ and also deeper than isolated $H_{BC}(0/+)$. This is in excellent agreement with the relative locations of the CH_I, CH_{II} and $E3'$ DLTS signals [9, 11, 12]. We also found that $CH_{BC4}(0/+)$ (where H sits at the fourth neighboring BC-site to the C atom) has a donor level at 0.22 eV below E_c, that is closer but still deeper than $H_{BC}(0/+)$ and also still below $H_{BC1}(-/0)$.

Following the suggestion of Ref. [13], that a CH_n complex (with $n > 1$) could be responsible for a donor level at $E_c - 0.14$ eV (labeled CH_B), we actually investigated that possibility for $n = 2$. We found that CH_2 can adopt two nearly degenerate configurations (within 30 meV) similar to that of H_2^* in Si, forming C-$H_{BC1} \cdots$ Si-$H_{AB(Si)}$ and $H_{AB(C)}$-C$\cdots H_{BC1}$-Si trigonal structures. The configuration with both H atoms bound to the C atom is metastable by 0.6–1 eV (depending on the charge state). We also found that the two lowest-energy structures are electrically inert, and therefore, should the $E_c - 0.14$ eV level belong to a CH_n complex, our results indicate that $n > 2$, most likely with one H atom located on a Si–Si bond.

4.2 Oxygen–hydrogen interactions Among the oxygen-hydrogen complexes investigated, those obtained after placing H next to interstitial O, as depicted in Fig. 2(b), had the lowest energy. While OH_{BC} is the ground state in the positive charge state, OH_{AB} was the most stable configuration in the negative charge state. The neutral defect is more stable with H at the BC-site (with OH_{AB}^0 being metastable by 0.23 eV only). We note that the H atom in OH_{BC} adopts a puckered configuration, making a Si-H-Si angle of 136° after structural relaxation. This means that some of the compressive strain, which is present in isolated Si-H_{BC}^+-Si and Si-O-Si defects along their 111 bond directions, is released in OH_{BC}^+ and that corresponds to a calculated binding energy of 0.30 eV. The binding energy of atomic H^- to interstitial O (with OH_{AB}^- as a reaction product) is estimated as 0.47 eV after considering independent supercells with H_T^- and O_i defects. Here, the negatively charged hydride ion establishes an ionic bond with the oxidized (positively charged) silicon atom that is connected to oxygen. The above figures match the experimentally determined binding energies of 0.29 and ~ 0.5 eV for defects which give rise to the $E3''$ and AT'' signals [10, 11], assigned to oxygen perturbed $(0/+)$ and $(-/0)$ transitions of bond-centered and tetrahedral hydrogen, respectively.

Further confirmation of the above model comes from the calculated electrical levels. In this case, isolated atomic H is expected to do a good job as marker. Accordingly, we place $OH_{BC}(0/+)$ and $OH_{T/BC}(-/0)$ transitions at $E_c - 0.16$ eV and $E_c - 0.69$ eV, respectively, in excellent agreement with the measured $E3''$ and AT'' signals with levels at $E_c - 0.17$ eV and $E_c - 0.68$ eV, respectively.

4.3 Carbon–oxygen–hydrogen complex In line with Ref. [7], we found that in the ground state of the CO complex, the O atom is located at the BC2-site with respect to carbon (see Fig. 2(a)). CO_{BC1} and CO_{BC4} configurations were metastable by 1.23 and 0.15 eV, respectively. The binding energy of CO_{BC2} (against formation of uncorrelated substitutional carbon and interstitial oxygen impurities) was found to be 0.51 eV. Inspection of the band structure revealed a clean band gap and no electrical levels were found.

The CO complex gives rise to three C-related LVM absorption bands at 589, 640, and 690 cm^{-1}, respectively 18 cm^{-1} below and 33 and 83 cm^{-1} above the unperturbed C_s-related triplet mode at 607 cm^{-1}. It also produces an O-related band at 1104 cm^{-1}, 32 cm^{-1} below the prominent 1136 cm^{-1} band from interstitial O [5, 6]. LVM frequency calculations for the CO_{BC2} model give C-modes at 557, 608, and 663 cm^{-1} plus one O-mode at 1074 cm^{-1}. The C-modes are 18 cm^{-1} below and 34, and 88 cm^{-1} above the calculated 575 cm^{-1} mode of isolated carbon. Analogously, we find the calculated O-mode frequency at 1074 cm^{-1}, 20 cm^{-1} below that of isolated O (calculated at 1094 cm^{-1}). These figures improve previous modeling results [7], account very well for the observations, and provide undisputable evidence for the correctness of the atomistic model.

For the interaction of H with CO, we found several low-energy configurations, which differ on the defect charge state. For a negatively charged COH (which should be stable under equilibrium in n-type material) we found that the structure shown in Fig. 3(a) and labeled COH_{AB}, is distinctly stable. Analogously to OH_{AB}^-, the H^- anion is attached to the electron-depleted Si atom, which in this case is further oxidized due to the bond with an electronegative C atom.

For the neutral defect, we found the COH_{BC1} configuration shown in Fig. 3(b) to be the ground state. COH_{AB}^0 is now metastable by 0.18 eV. The BC1 structure is made of a CH_{BC1} defect perturbed by a nearby interstitial O atom, so it is expected to show rather similar electronic properties to CH_{BC1}. Another low energy configuration was COH_{BC2}^0 (0.05 eV above the ground state), which is depicted in Fig. 3(c).

Finally, for positively charged COH, the ground state configuration is now COH_{BC2} (Fig. 3(c)), which resembles an OH_{BC}^+ complex stabilized by a nearby tensile C_s defect. Another stable structure is COH_{BC1}^+ (0.08 eV above the BC2 ground state).

Now we proceed to the calculation of the electrical levels of COH. On this report, we will focus on the acceptor activity only. Accordingly, the relevant acceptor transitions are $COH_{AB}(-/0)$, $COH_{AB/BC1}(-/0)$ and $COH_{AB/BC2}(-/0)$. While the last two involve electronic states similar to that of the $H_{T/BC}(-/0)$ marker, the $COH_{AB}(-/0)$ direct transition finds no resemblance with either $H_{T/BC}(-/0)$ or $VOH(-/0)$. Conversely, the $OH_{AB}(-/0)$ transition (observed at $E_c - 0.79$ eV [11]) should closely describe the $COH_{AB}(-/0)$ level. Hence, we obtain indirect $COH_{AB/BC1}(-/0)$ and $COH_{AB/BC2}(-/0)$ levels at $E_c - 0.81$ eV and $E_c - 0.76$ eV, respectively, that is, $E_v + 0.31$ eV and $E_v + 0.36$ eV if we consider 1.12 eV for the band gap of Si. We also find a direct $COH_{AB}(-/0)$ at $E_c - 0.80$ eV.

Although all three calculated levels agree very well with the location of the H_1/H_2 hole traps, we note that we have

Table 1 Calculated (calc) and experimental (exp) electronic levels of the defects investigated in this work. All values are given in eV.

electronic level	calc	exp
$E_c - CH_{BC1}(-/0)$	0.17	0.16 [12]
$CH_{BC1}(0/+) - E_v$	0.28	0.33 [12]
$E_c - CH_{BC2}(0/+)$	0.24	0.22 [12]
$E_c - OH_{AB/BC}(-/0)$	0.69	0.68 [11]
$E_c - OH_{BC}(0/+)$	0.16	0.17 [10]
$E_c - COH_{AB}(-/0)$	0.80	
$E_c - COH_{AB/BC1}(-/0)$	0.81	
$E_c - COH_{AB/BC2}(-/0)$	0.76	

two rather different mechanisms that could explain the recombination activity. These are (i) a direct $COH_{AB}(-/0)$ transition, or (ii) a mechanism involving indirect $COH_{AB/BC1}(-/0)$ and $COH_{AB/BC2}(-/0)$ levels which imply a structural change in the neutral charge state. A deeper understanding of the above processes will involve the calculation of the potential energy surface between the AB, BC1, and BC2 configurations. We leave this for a future report to be published elsewhere.

The structural distinction between the H_1 and H_2 traps is also an open question. Until now, we have considered the interactions between single C, O, and H species. It is possible that one of these traps involves two O or H atoms, and we intend to look at this problem in the near future.

5 Conclusions We presented a joint theoretical and experimental study of the interaction of H with carbon- and oxygen-related defects in silicon. For convenience, we summarize all calculated levels and experimental assignments in Table 1.

We started by reporting on the interaction of H with a C_s impurity, where based on the total energies and calculated levels, we confirm the support from first-principles theory to the assignment of CH_{II} and CH_I DLTS signals in Ref. 12 to carbon-hydrogen defects with the H atom on the first- and second-neighboring BC sites with respect to a C_s impurity, respectively. We did not find any CH defect with two or less H atoms, which could give rise to a donor transition above $H_{BC}(0/+)$. This suggests that the CH_B level at $E_c - 0.14$ eV reported in Ref. [13] could be related to a CH_n complex involving $n > 2$ hydrogen atoms.

The calculations support the interpretation of earlier experimental work [11], according to which H can bind to interstitial oxygen to from either OH^+ or OH^- with negative-U ordering of the donor and acceptor levels. We found that for the positive charge state H is nearly bond-centered forming a $Si-H_{BC}^+-Si-O_i-Si$ zig-zag chain (like the O-dimer in Si), while the negative defect adopts an anti-bonding configuration that results in a nearly trigonal H_{AB}^--Si-O-Si linear defect. The calculated binding energies and electrical levels are in excellent agreement with the observations.
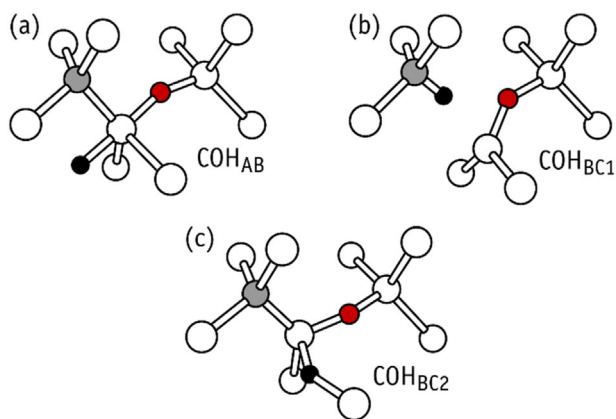

Figure 3 Ground state structures for COH in the negative (a), neutral (b), and positive (c) charge states. Si, C, O, and H atoms are shown in white.

Phys. Status Solidi A 214, No. 7 (2017)

Original
Paper

(6 of 6) 1700309

We finally investigated the CO complex and its interaction with H. We confirm that C and O atoms in CO are bound to a common Si atom − no direct C–O bond is established. The calculated local vibrational mode frequencies for this complex account very well for all four bands observed by infra-red absorption measurements.

The COH complex is predicted to adopt different configurations in all three charge states that were investigated ($-$, 0, and $+$). In the negative charge state, and particularly in n-type material, the complex takes the form of an OH_{AB}^- defect perturbed by a nearby C_s impurity, being therefore referred to as COH_{AB}^-. We suggest that this structure, shown in Fig. 3(a), corresponds to the observed hole-trapping center reported in Section 3. The neutral charge state was found to have several virtually degenerate configurations with the H atom either connected to the C atom, or at a nearby BC site (see Fig. 3(b) and (c)). Several calculated electrical levels are close to the observed H_1/H_2 traps, although further work is needed in order to understand eventual defect transformations upon carrier trapping/emission events.

References

[1] R. Jones (Ed.), Early stages of oxygen precipitation in silicon, in: NATO Advance Science Institutes, Series 3: High Technology, Vol. 17 (Kluwer Academic, Dordrecht, 1996), https://doi.org/10.1007/978-94-009-0355-5

[2] R. C. Newman and R. Jones, Curr. Opin. Solid State Mater. Sci. **2**, 40–47 (1997). https://doi.org/10.1016/S1359-0286(97)80103-9

[3] S. K. Estreicher, M. Stavola, and J. Weber, Hydrogen in Si and Ge, in Silicon, Germanium, and Their Alloys: Growth, Defects, Impurities, and Nanocrystals, edited by G. Kissinger and S. Pizzini (CRC, Boca Raton, 2015), pp. 217–254.

[4] F. Duerinckx and J. Szlufcik, Sol. Energy Mater. Sol. Cells **72**, 231 (2002). https://doi.org/10.1016/S0927-0248(01)00170-2

[5] R. C. Newman and J. B. Willis, J. Phys. Chem. Solids **26**, 373–379 (1965). https://doi.org/10.1016/0022-3697(65)90166-6

[6] A. R. Bean and R. C. Newman, J. Phys. Chem. Solids **33**, 255–268 (1972). https://doi.org/10.1016/0022-3697(72)90004-2

[7] C. Kaneta, T. Sasaki, and H. Katayama-Yoshida, Phys. Rev. B **46**, 13179 (1992). https://doi.org/10.1103/PhysRevB.46.13179

[8] B. Holm, K. Bonde Nielsen, and B. Bech Nielsen, Phys. Rev. Lett. **66**, 2360 (1991). https://doi.org/10.1103/PhysRevLett.66.2360

[9] N. M. Johnson, C. Herring, and C. G. Van de Walle, Phys. Rev. Lett. **74**, 1889 (1995). https://doi.org/10.1103/PhysRevLett.74.1889

[10] K. Bonde Nielsen, B. Bech Nielsen, J. Hansen, E. Andersen, and J. U. Andersen, Phys. Rev. B **60**, 1716 (1999). https://doi.org/10.1103/PhysRevB.60.1716

[11] K. Bonde Nielsen, L. Dobaczewski, S. Søgård, and B. Bech Nielsen, Phys. Rev. B **65**, 075205 (2002). https://doi.org/10.1103/PhysRevB.65.075205

[12] O. Andersen, A. R. Peaker, L. Dobaczewski, K. Bonde Nielsen, B. Hourahine, R. Jones, P. R. Briddon, and S. Öberg, Phys. Rev. B **66**, 235205 (2002). https://doi.org/10.1103/PhysRevB.66.235205

[13] R. Stübner, V. Kolkovsky, and J. Weber, J. Appl. Phys. **118**, 055704 (2016). https://doi.org/10.1063/1.4928146

[14] S. K. Estreicher, Phys. Rev. B **41**, 9886 (1990). https://doi.org/10.1103/PhysRevB.41.9886

[15] R. Jones, S. Öberg, and A. Umerski, Mater. Sci. Forum **83-87**, 551 (1992). https://doi.org/10.4028/www.scientific.net/MSF.83-87.551

[16] S. K. Estreicher, Early stages of oxygen precipitation in silicon, in: NATO Advance Science Institutes, Series 3: High Technology, Vol. 17, edited by R. Jones (Kluwer Academic, Dordrecht, 1996), pp. 179–195. https://doi.org/10.1007/978-94-009-0355-5

[17] M. Vaqueiro-Contreras, V. P. Markevich, M. Halsall, A. R. Peaker, P. Santos, J. Coutinho, S. Öberg, L. Murin, R. Falster, J. Binns, E. Monakhov, and B. G. Svensson, to appear in Phys. Status Solidi RRL.

[18] R. Brunwin, B. Hamilton, P. Jordan, and A. R. Peaker, Electron. Lett. **15**, 349 (1979). https://doi.org/10.1049/el:19790248

[19] G. Kresse and J. Furthmüller, Comput. Mater. Sci. **6**, 15 (1996). https://doi.org/10.1016/0927-0256(96)00008-0

[20] P. E. Blöchl, Phys. Rev. B **50**, 17953 (1994). https://doi.org/10.1103/PhysRevB.50.17953

[21] J. P. Perdew, K. Burke, and M. Ernzerhof, Phys. Rev. Lett. **77**, 3865 (1996). https://doi.org/10.1103/PhysRevLett.77.3865

[22] A. Resende, R. Jones, S. Öberg, and P. R. Briddon, Phys. Rev. Lett. **82**, 2111 (1999). https://doi.org/10.1103/PhysRevLett.82.2111

[23] J. Coutinho, O. Andersen, L. Dobaczewski, K. Bonde Nielsen, A. R. Peaker, R. Jones, S. Öberg, and P. R. Briddon, Phys. Rev. B **68**, 184106 (2003). https://doi.org/10.1103/PhysRevB.68.184106

[24] L. Kimerling and J. Benton, Appl. Phys. Lett. **39**, 410 (1981). https://doi.org/10.1063/1.92755

[25] M. Yoneta, Y. Kamiura, and F. Hashimoto, J. Appl. Phys. **70**, 1295 (1991). https://doi.org/10.1063/1.349586

[26] Y. Tokuda, I. Katoh, H. Ohshima, and T. Hattori, Semi. Sci. Tech. **9**, 1733 (1994). https://doi.org/10.1088/0268-1242/9/9/026

[27] V. P. Markevich, M. Vaqueiro Contreras, J. Mullins, M. Halsall, B. Hamilton, L. I. Murin, R. Falster, J. Binns, E. Good, J. Coutinho, J. Medford, C. L. Reynolds Jr., and A. R. Peaker, 2016 IEEE 43rd Photovoltaic Specialists Conference (PVSC), (Portland, 2016), pp. 0688–0693. https://doi.org/10.1109/PVSC.2016.7749689